Pergamon

Bioorganic & Medicinal Chemistry 10 (2002) 79–85

BIOORGANIC & MEDICINAL CHEMISTRY

Medium-Dependence of the Secondary Structure of Exendin-4 and Glucagon-like-peptide-1

Niels H. Andersen,[a,*] Yan Brodsky,[a] Jonathan W. Neidigh[a] and Kathryn S. Prickett[b]

[a]*Department of Chemistry, University of Washington, Seattle, WA 98195, USA*
[b]*Amylin Pharmaceuticals Inc., 9373 Towne Centre Drive, San Diego, CA 92121, USA*

Received 25 April 2001; accepted 2 July 2001

Abstract—Exendin-4 is a natural, 39-residue peptide first isolated from the salivary secretions of a Gila Monster (*Heloderma suspectum*) that has some pharmacological properties similar to glucagon-like-peptide-1 (GLP-1). This paper reports differences in the structural preferences of these two peptides. For GLP-1 in aqueous buffer (pH 3.5 or 5.9), the concentration dependence of circular dichroism spectra suggests that substantial helicity results only as a consequence of helix bundle formation. In contrast, exendin-4 is significantly helical in aqueous buffer even at the lowest concentration examined (2.3 μM). The pH dependence of the helical signal for exendin-4 indicates that helicity is enhanced by a more favorable sequence alignment of oppositely charged sidechains. Both peptides become more helical upon addition of either lipid micelles or fluoroalcohols. The stabilities of the helices were assessed from the thermal gradient of ellipticity ($\partial[\theta]_{221}/\partial T$ values); on this basis, the exendin helix does not melt appreciably until temperatures significantly above ambient. The extent of helix formation for exendin-4 in aqueous buffer (and the thermal stability of the resulting helix) suggests the presence of a stable helix-capping interaction which was localized to the C-terminal segment by NMR studies of NH exchange protection. Solvent effects on the thermal stability of the helix indicate that the C-terminal capping interaction is hydrophobic in nature. The absence of this C-capping interaction and the presence of a flexible, helix-destabilizing glycine at residue 16 in GLP-1 are the likely causes of the greater fragility of the monomeric helical state of GLP-1. The intramolecular hydrophobic clustering in exendin-4 also appears to decrease the extent of helical aggregate formation.

Introduction

Diabetes mellitus is a chronic disease characterized by multiple metabolic abnormalities arising primarily from an inadequate insulin effect. Glucagon-like peptide-1 (GLP-1),[1] a mammalian hormone, has been investigated as a potential therapeutic agent for the treatment of this disease because of its favorable spectrum of antidiabetic actions which include a glucose dependent insulinotropic action,[2,3] an effect to modulate gastric emptying[4] and a possible role in appetite control.[5] GLP-1 mimics also have potential as an obesity treatment.[6] Due to its short duration of action, however, GLP-1 may have limitations as a therapeutic agent.

Exendin-4 is a natural, 39-residue peptide[7] that displays greater than 50% sequence identity to GLP-1. Exendin-4 has been shown to bind and act as an agonist at the GLP-1 receptor on prepared RINm5f cell membranes[8] and to have activities known to be important for improvement of glucose control, including stimulation of insulin secretion and modulation of gastric emptying. AC2993 (synthetic exendin-4) has been shown to be markedly more potent and/or long-lived in vivo than GLP-1 for these activities.[9] AC2993 is currently in phase 2 clinical trials as a treatment for type 2 diabetes. GLP-1 and exendin-4 also have significant homology to glucagon. The sequences are shown below.

Exendin-4	HGEGTFTSDL SKQMEEEAVR LFIEWLKNGG PSSGAPPPS-NH_2
GLP-1	HAEGTFTSDV SSYLEGQAAK EFIAWLVKGR-NH_2
Glucagon	HSQGTFTSDY SKYLDSRRAQ DFVQWLMNT

The literature contains numerous structural studies of glucagon, a few of GLP-1, but none for exendin-4. Only the helical states of glucagon have been well characterized by, for example, X-ray crystallography[10] and NMR in the micelle-associated state.[11] We and others[12] have examined glucagon by circular dichroism (CD). The CD studies reveal a solvent and concentration dependent

*Corresponding author. Tel.: +1-206-543-7099; e-mail: andersen@chem.washington.edu

0968-0896/02/$ - see front matter
PII: S0968-0896(01)00263-2

conformational equilibrium with significant helicity in the micelle-associated state; however, glucagon is only ca. 15% helical in water and forms 'soluble' β sheet aggregates with time at concentrations $\geq 100\,\mu M$. GLP-1 has been examined by NMR in aqueous media containing dodecylphosphocholine (DPC) micelles;[13] the resulting NMR structure ensemble is helical from residue 7 to 29 with distortions in backbone helix geometry near Gly[16]. The authors suggested that this helix distortion could be important for both membrane and receptor binding. Glucagon, which otherwise displays significant homology to GLP-1, lacks the flexible linker induced by Gly[16] and displays diminished binding to GLP-1 receptors.[3] However, exendin-4 also lacks the flexible linker, having MEEE in place of the central LEGQ segment of GLP-1, and yet has potent antidiabetic actions. Parker et al.[14] have presented NMR structures and potency data for covalently cross-linked GLP-1 analogues, suggesting that the C-terminal helix of GLP-1 is essential for the display of pharmacophore components. Based on this, we have compared the structuring preferences of GLP-1 and exendin-4; CD studies in both the solution state and in the presence of lipid micelles are presented here as well as a preliminary NMR determination of the helix stability of exendin-4.

Results

At peptide concentrations $>40\,\mu M$, the CD spectra of both GLP-1 and exendin-4 in aqueous buffer were time dependent. However, we did not observe, at any time point or concentration, a β sheet CD signature as we had previously observed for glucagon at high concentrations in the absence of fluoroalcohol or lipid additives. The aggregation observed with GLP-1 (and to a lesser extent with exendin-4) does not appear to represent the formation of β sheet species.

At pH 5.9, the helix signature of exendin-4 diminishes slightly over a 2–4 day period. At pH 3.5, there is a 33% drop in the $-[\theta]_{221}$ value over 24 h. Even after these losses in net $-[\theta]_{221}$ signal, the CD traces show no significant change in the characteristic intensity ratios of the three extrema ($\lambda = 191$, 208, 221 nm). These observations suggest the formation of non-soluble aggregates that adhere to the walls of the glass vials used to store the CD samples during the stability studies. Irreversible aggregation is less of a problem with GLP-1 at pH 3.5. With GLP-1, irreversible aggregation and adsorption is observed at pH 5.9 but at a slower rate than observed for exendin-4; a six-day period is required for a comparable reduction of the CD signal. The CD spectra of GLP-1 and exendin-4 in aqueous buffer at concentrations where aggregation is not present and the spectrum of the helical state of exendin-4 formed upon fluoroalcohol addition are shown in Figure 1.

Turning to CD data recorded immediately after peptide dissolution, Table 1 summarizes the $-[\theta]_{221}$ values for exendin-4 and GLP-1 in all media examined. Coiled coil formation should occur on a minutes-or-faster timescale and is thus expected to be fully reflected in this data but the data should be free of contributions from slowly formed aggregates. The concentration dependence of $[\theta]_{221}$ in aqueous buffer (Table 1A) suggests that the modest helicity displayed by GLP-1 is due to coiled coil (or other helix bundle) formation. At the lowest concentration examined, the pH 5.9 CD spectrum of GLP-1 suggests a very small helicity for the monomeric state, even though coiled coil formation occurs readily at higher concentrations at this pH. For exendin-4, there is only a modest increase in $-[\theta]_{221}$ with concentration at pH 5.9. If significant oligomer formation occurs at higher concentrations, the CD spectrum of the resulting bundle state must be very similar to that of the monomeric species. At pH 3.5, some helicity enhancement by oligomerization is evident (Table 1A). Exendin-4 displays substantial helicity in aqueous pH 5.9 buffer even at 2.3 μM peptide concentrations. At pH 4.5–5.9, exendin-4 appears to favor a monomeric helical state throughout the 2–230 μM concentration range, although some degree of helical aggregate formation may occur at the highest concentration.

GLP-1 and exendin-4 both become more helical in media containing lipid micelles (Table 1B) and the concentration dependence of $-[\theta]_{221}$ disappears indicating that the peptides are monomeric under these conditions. A further increase in helicity occurs (particularly for GLP-1) in aqueous fluoroalcohol media (Table 1C). We assumed a common residue 7–28 helical span for both peptides (the largest possible one based on helix prediction algorithms,[15,16] vide infra) to convert the CD data to fractional helix populations (χ_{helix}). These values appear in the last column of Table 1. In aqueous fluoroalcohol media, other portions of both sequences must either become helical or structured in some other way that contributes to the negative $[\theta]_{221}$ value (by type I/III turn formation, for example). This is most notable for exendin-4, which has a higher proportion of its total sequence outside of the predicted helical span.

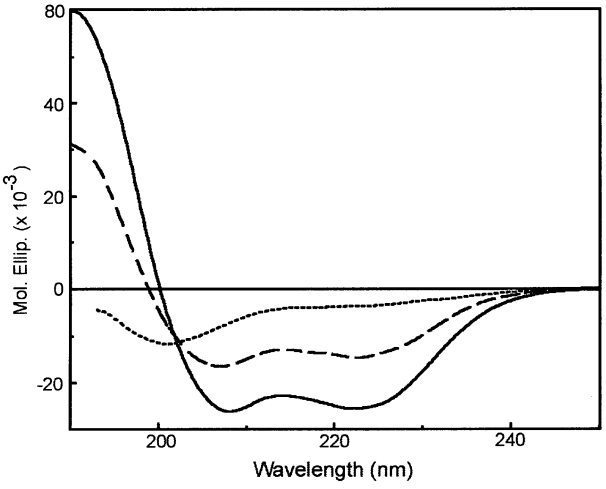

Figure 1. Representative far UV CD spectra at 21 °C: listed in order of increasingly negative values of $[\theta]_{221}$: a) least helical, dotted line (· · · ·), 3.15 μM GLP-1 in pH 5.9 buffer; b) dashed line (- - - -), 2.3 μM exendin-4 in pH 5.9 buffer; and c) most helical, solid line (———), 28.5 μM exendin-4 in 25% HFIP.

Curve shape analysis, as expressed in ellipticity ratios (R1 and R2), has emerged as an alternative measure of fractional helicity.[17] These measures (appearing in Table 2) confirm the %-helicities obtained from the absolute $[\theta]_{221}$ values. At 0 °C, the ellipticity ratios observed for exendin-4 in 25% HFIP or 40% TFE are within the expectation range for 100% helicity suggesting that the non-structured portions of the sequence are making little net contribution to the far UV CD signal. This provides additional support for using $[\theta]_{221}$ values as a measure of the fractional helicity over the helical span.

Although there is still some controversy regarding the $[\theta]_{221}$ value that corresponds to 100% helicity at high temperatures, particularly when fluoroalcohols are present,[18] the thermal gradient of $[\theta]_{221}$ can still serve as a measure of helix stability. Two representative melting studies appear in Figure 2. We adopted the %-loss of $-[\theta]_{221}$ signal on warming from 0 to 20 °C as the measure of the thermal stability of the GLP-1 and exendin helices in different media, Table 3. Exendin-4 displays less thermal helicity loss than GLP-1 under all conditions except in 25% HFIP. This is particularly notable in aqueous buffer (8.8% loss at pH 3.5) and in 8% HFIP (6% helicity loss).

To place these signal losses in context, we note that helical proteins display $-[\theta]_{221}$ signal losses for $\Delta T = 20$ °C as small as 2.8% below their T_m values. Literature values for the intrinsic gradient for 100% helicity for peptides in water imply that signal loss values of 5%[19] to 11%[18] represent no net loss of helicity. By any of these criteria, the exendin helix appears to be unusually stable. In contrast, the limited helicity of GLP-1 melts out rapidly on warming. At pH 5.9, the helix loss at 50 μM is largely attributable to disaggregation. The ready thermal loss of the limited helicity observed at pH 3.5 is attributed to GLP-1 monomers.

Additional evidence for the stability of the exendin-4 helix comes from an NMR study that revealed surprisingly large exchange protection factors for the backbone NHs of Ile[23], Glu[24], Trp[25] and Leu[26]. The NOESY spectrum panel in Figure 3 illustrates this. The exendin-4 sample examined had spent more than 16 h in 15 mM phosphate buffered D_2O (pH* 5.3) at 21 °C before the final lyophilization prior to NMR sample preparation. The NH resonances of the listed residues displayed 0.4–0.8^+ fractional proton occupancy while all of the remaining NHs were essentially absent from the spectrum. This degree of exchange protection requires fractional helicities in excess of 0.97 in the two C-terminal turns of the helix.

Discussion

Based on the time-dependent CD data neither GLP-1 nor exendin-4 form β aggregates as is routinely observed for glucagon in aqueous buffer at high concentrations. Significant helix formation for GLP-1 in water is largely the result of coiled coil (or other helix bundle) forma-

Table 1. Circular dichroism data for exendin-4 and GLP-1

	Conditions	Conc. (μM)		$-[\theta]_{221}$		χ^{helix}	
		Exendin-4	GLP-1	Exendin-4	GLP-1	Exendin-4	GLP-1
A	Aqueous buffer, pH 3.5	2.3	3.15	11,370	5700	**0.55**	0.23
	Aqueous Buffer, pH 3.5	28.5	50	14,900	6560	**0.70**	0.26
	Aqueous Buffer, pH 3.5		315		8900		0.34
	Aqueous Buffer, pH 5.9	2.3	3.15	14,500	3670	0.69	**0.15**
	Aqueous Buffer, pH 5.9	28.5	50	16,100	9980	0.76	**0.38**
	Aqueous, pH 4.5	228		17,600		0.83	
B	13 mM SDS, pH 3.5	28.5	50	17,000[a]	23,700	0.83	0.85
	13 mM SDS, pH 5.9	28.5	50	16,200[a]	19,700	0.79	0.71
	30 mM octyl-Glu, pH 3.5	Not soln	50		24,850		0.89
	30 mM octyl-Glu, pH 5.9	Not soln	50		20,670		0.75
	40 mM C_{12}-PC, pH 3.5	28.5	50	18,100	20,200	0.85	0.73
	40 mM C_{12}-PC, pH 3.5	200	270	18,000	19,800	0.84	0.72
	40 mM C_{12}-PC, pH 5.9	28.5	50	17,900	17,050	0.84	0.62
	40 mM C_{12}-PC, pH 5.9	200	270	19,200	18,050	0.90	0.65
C	8% HFIP, pH 3.5	28.5	50	20,000	25,650	0.93	0.92
	40% TFE, pH 3.5	28.5	50	23,700	28,880	1.10[b]	1.03[b]
	25% HFIP, pH 3.5	28.5	50	25,500	32,560	>1.1[b,c]	>1.1[b,c]
D	Calcd for $\chi_{helix} = 1.00$			21,500	28,000		
	Calcd for $\chi_{helix} = 0.00$			−800	−830		

The $-[\theta]_{221}$ values for exendin-4 and GLP-1 in the various types of media (A, B, C) employed in this study are presented (at room temperature, 21 ± 2 °C, except as noted). The calculation of expectation values (D) for the helical and coil states of exendin-4 and GLP-1 employed formula and corrections for aromatic chromophores[16] in calculating θ_C and θ_H values at 0 °C. A common helical segment, residues 7–28, was assumed along with helix and coil temperature gradients of −65°/°C and +65°/°C at λ = 221 nm, respectively, for calculating the fractional helicity (χ_{helix}) over that span. Instances of large χ_{helix} differences between exendin-4 and GLP-1 are highlighted in bold.

[a]Experiments performed at 37 °C to improve solubility.

[b]Since the helix population calculations assumed a common 7–28 helical segment, calculated values greater than 1.00 suggests that helicity can be induced in the C-terminal proline-rich segment of exendin-4 at high fluoroalcohol levels.

[c]In 25% HFIP, both peptides display $-[\theta]_{221}$ values that are significantly greater than those expected for a residue 7–28 helical span (given in **D**). Apparently HFIP induces additional helicity (or helix-like turns) in the N-terminal portions of both sequences.

Table 2. Ellipticity ratios for exendin-4 and GLP-1 in different media

Conditions	Conc. (μM)		R1[a]		R2[a]	
	Exendin-4	GLP-1	Exendin-4	GLP-1	Exendin-4	GLP-1
Aqueous buffer, pH 3.5	28.5	50	−1.73	−0.10	+0.79	+0.43
Aqueous buffer, pH 5.9	28.5	50	−1.82	−1.01[b]	+0.86	+0.68[b]
40 mM C_{12}-PC, pH 3.5	28.5	50	−1.60	−2.07	+0.72	+0.87
40 mM C_{12}-PC, pH 5.9	28.5	50	−1.67	−2.08	+0.73	+0.85
40% TFE or 25% HFIP	28.5	50	−2.21	−1.92	+0.97	+0.85
same media at 0 °C	28.5	50	−2.34±0.04	−2.07	+1.05±0.02	+0.90
$\chi_{helix} = 1.00$ Expectation values			−2.45±0.25		+1.06±0.05	
$\chi_{helix} = 0.00$ Expectation values			+0.65±0.15		−0.03±0.05	

The ratios are at 21 °C, except as noted. The last entries are the expectation values for 0 and 100% helicity. The peptide and conditions are listed for the other entries.

[a]The ellipticity ratios employed are defined here. $R1 = [\theta]_{max}/[\theta]_{min}$ and $R2 = [\theta]_{221}/[\theta]_{min}$, where $[\theta]_{min}$ refers to the minimum at 197–210 nm and $[\theta]_{max}$ is the most positive ellipticity observed in the 190–195 nm span..[17]

[b]The dramatic increase toward helical values at pH 5.9 is rationalized as the result of coiled coil formation which is enhanced with increasing pH.

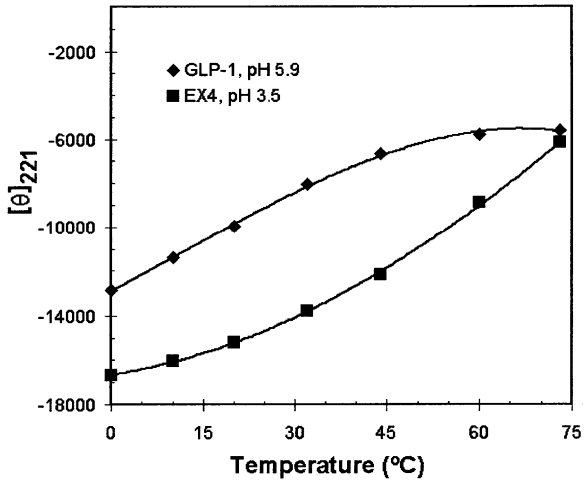

Figure 2. Thermal melting curves for exendin-4 and GLP-1 in aqueous buffer: circular dichroism ($[\theta]_{221}$) versus temperature. Freshly prepared stock solutions were diluted to 28.5 μM (exendin-4) and 50 μM (GLP-1) with phosphate/acetate buffer of the pH indicated in the legend in the figure inset. The room temperature $[\theta]_{221}$ values were recovered upon cooling from the highest temperature examined.

tion. However, all of the evidence presented suggests that exendin-4, unlike GLP-1 or glucagon, forms a monomeric helical state in aqueous media. While exendin-4 may still have some tendency to aggregate at higher concentrations, aggregation is not required for helix formation. The exendin sequence results in a better alignment of alternating negative and positive side-chains on one face, which can stabilize the helix via salt-bridging or polar H-bonds. For exendin-4, monomeric helix stabilization is clearly enhanced by glutamate ionization as evidenced by the pH effect on $[\theta]_{221}$ (see Table 1A). This stabilizing feature continues to contribute in the DPC micelle-associated state, but to a lesser degree. In fluoroalcohol-containing media, the pH differences are virtually absent (data not shown). The diminished helicity of GLP-1 in the DPC micelle system relative to that of exendin-4 may be attributable to helix disruption at the Gly^{16} locus of GLP-1. However glucagon, which lacks a helix disrupting residue and has a better sequence alignment for salt bridging (see Fig. 5, vide infra), is also less helical than exendin-4 in the monomeric state. Since both helix disruption by glycine and helix stabilization by coulombic and hydrophobic interactions should be modeled by current helicity prediction algorithms, we employed AGADIR[20] and Helix1.5[16,21] to derive predicted helicity profiles for these peptides (Fig. 4).

Both algorithms predict that the N-terminal residues of exendin-4 and GLP-1 are unstructured in solution even though they are required for pharmacological activity.[22] The lesser net helicity of GLP-1 is clearly evident in the predicted helicity profiles from both algorithms. The two algorithms predict quite different N-capping effects, but in each case the decreased helix propensity of GLP-1 can be attributed to Gly.[16] These parameterization differences are also reflected in the predicted histograms of helicity along the sequence of exendin-4; the AGADIR algorithm appears to weight coulombic and hydrophobic side-chain interactions more heavily and predicts greater helicity than Helix1.5, particularly for the C-terminal segment. The AGADIR prediction is more nearly in accord with the experimental determination (0.61 over residues 7–28 vs 0.69 as observed by CD). However, AGADIR fails to rationalize the localization of NH exchange protection to the extreme C-terminus (residues 23–26, as evidenced by Figure 3). The AGADIR algorithm predicts residue fractional helicities between 0.825 and 0.872 from Glu^{17} through Leu^{26} at the temperature of CD data reported in Table 1. The same temperature was employed for the D_2O exchange study. Based on the AGADIR helicity profile, comparable NH protection would be expected from Val^{19} to Leu^{26}; this is not observed. Furthermore, the degree of exchange protection observed for Ile^{23}–Leu^{26} at 293 K requires fractional helicities of 0.97 or greater at residues 21–24.

The folding cooperativity and thermal stability of the exendin-4 helix in aqueous buffer suggests the presence of a stable helix-capping interaction. The thermal stability is even more pronounced in 8 vol% HFIP suggesting that the helix stabilization is a hydrophobic effect.[23] Since the only significant polar/apolar sequence differences between exendin-4 and GLP-1 are the hydrophobic

Table 3. Helix melting as measured by %-loss of $-[\theta]_{221}$ signal on warming from 0 to 20 °C

Medium	GLP-1	Exendin-4
	%-loss	%-loss
Aqueous buffer, pH 3.5	30	8.8
Aqueous buffer, pH 5.9	22	12.7
8% HFIP	12	6.0
25% HFIP	10.3	10.6
40% TFE	12.5	11.0

side-chain at position 21 and the non-helical proline-rich C-terminal extension present only in exendin-4, the source of the unexpected helix stabilization should be sought in this region. NMR studies of single site mutations in this sequence and of the structuring preferences associated with the introduction of the C-terminal segment of exendin are in progress.

Does this study increase our understanding of the features required for in vitro GLP-1 receptor binding and activation? For peptides with conformational versatility, there is always reason to doubt that any particular structural feature or structuring preference observed in any state other than the receptor-bound state can be used to derive the requisites for receptor binding and activation. In the present case, however, the C-terminal portion of a helix has now been observed for the DPC micelle-associated states of GLP-1 and exendin-4, in the solution-state for exendin-4, and for active covalently constrained GLP-1 analogues.[14] DPC micelles may mimic the membrane context of the peptides just prior to binding to the receptor. The greater intrinsic stability of the exendin helix should reduce the entropic cost of binding at a receptor that requires the C-terminal helix state,[14] thus increasing the affinity for the receptor. The appropriately displayed residues of the C-terminal helix likely represent receptor binding requirements. The N-terminal residues including His[1] and Phe[6] are known to be essential for agonist activity and the spatial relationship between these signaling requirements and the C-terminal binding unit is more difficult to assess.

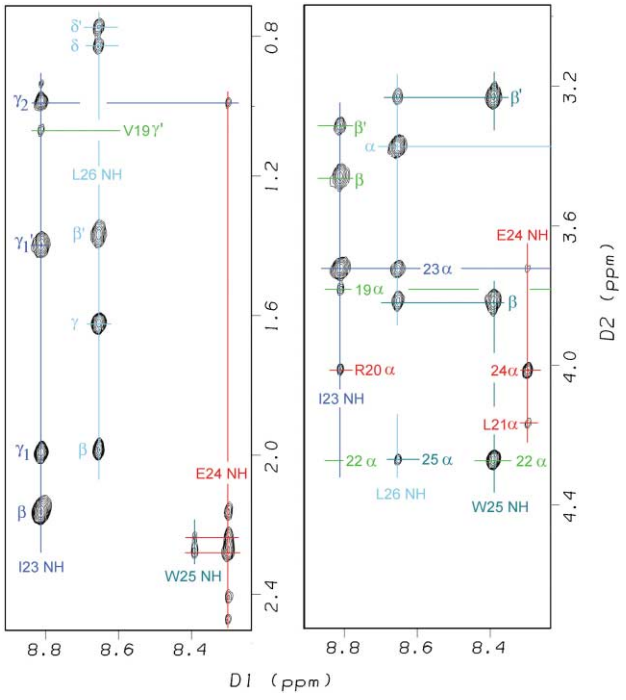

Figure 3. Panels showing the NH region of the $\tau_m = 150$ ms NOESY spectrum of exendin-4 in 30% d_3-TFE/70% D_2O buffer (pH* = 5.9) at 300K after extensive prior exchange in buffered 99.9 + % D_2O (pH* adjusted to 5.35). Subsequent experiments in protic media establish that the NHs of Val[19], Leu[21] and Phe[22] appear at 8.06, 8.42, and 8.32 ppm; these are entirely absent in this D_2O exchanged sample. NOESY cross peaks that serve to confirm the assignment and establish that this is a helical segment are labeled and color coded by residue. The Phe[22]-Hα (4.292 ppm) and Trp[25]-Hα (4.281 ppm) signals are nearly shift coincident; Arg[20]-Hα and Glu[24]-Hα are shift coincident (δ = 4.014 ppm). A weak 22Hα/23HN NOESY peak appears when the spectrum is plotted with a lower contour level cut-off. No additional cross-peaks to NH frequencies were observed, even at lower contour levels.

Amphiphilic character and the alignment of the aryl sidechains—F6, Y13 (not present in exendin-4), F22, and W25—on a single helix face has been proposed[13] as a key feature for membrane binding. The absence of this feature (in GLP-1, glucagon and exendin-4) in a helical structure spanning this entire segment is evident in helix wheel depictions of these peptides (Fig. 5). The present study reveals that the helix disrupting effect of Gly[16] is even greater than previously suggested;[13] more amphiphilic conformations are certainly accessible for GLP-1. Helix distortions would be less likely in exendin-4 (**D**), the Gly[16] to Ala mutant of GLP-1 (**A**), and upon deletion (**B**) of Gly[16]. The potency effects of modifications at Gly[16] have been determined. The Gly[16] to Ala mutant of GLP-1 binds to RINm5F cell receptor equally as well as GLP-1[24] and show only slightly diminished activity.[22] Deletion of Gly[16], however, produces a 40-fold loss in binding affinity[14] even though this change does create a more amphiphilic helix (**B**) with all of the aryl groups clustered together. In some support for the amphiphilic

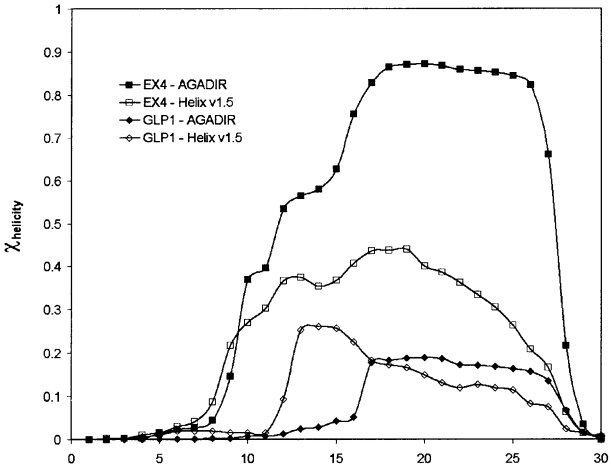

Figure 4. Comparison of the residue histograms of predicted helicity at pH 6 (293K) for exendin-4 and GLP-1 using the AGADIR and Helix1.5 algorithms. The more completely parameterized AGADIR algorithm predicts greater helicity for the amphiphilic exendin system. For comparison with Table 1, the predicted helicities for residues 7–28 at 294 K are 0.097 for GLP-1 and 0.60 for exendin-4 using the AGADIR algorithm.

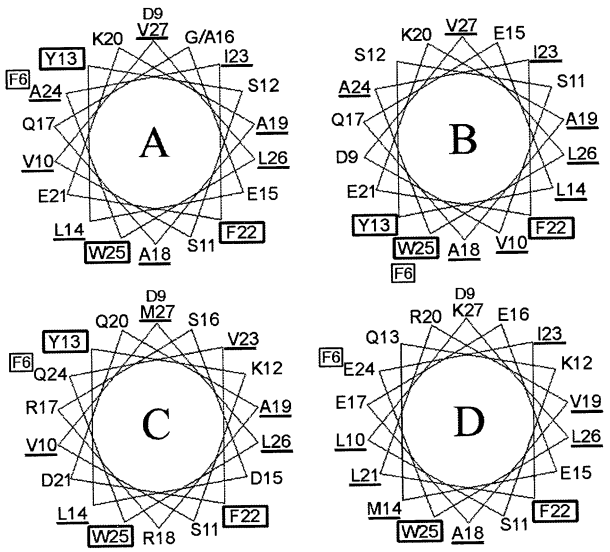

Figure 5. Helix wheel representations of (G16A)-GLP-1 (**A**), (desG16)-GLP-1 (**B**), glucagon (**C**) and exendin-4 (**D**) retaining the same orientation relative to F22 and W25. Non-polar residues are underlined; aromatic residue symbols are enboxed. This representation, which assume a perfect α-helix conformation, is unlikely to be appropriate for unmodified GLP-1 even in a membrane-mimicking micelle system.

helix hypothesis, the E/D21L change versus GLP-1 and glucagon (and the R18A change vs glucagon) does result in a more uniformly hydrophobic face in exendin-4. However, at this point the only feature of the receptor bound state that can be confidently predicted is the C-terminal helix. Hypotheses concerning the spatial relationship of the C-terminal helix to signaling requisites near the N-terminus would be speculation at this point.

Experimental

Exendin-4 and GLP-1 were prepared by standard solid-phase peptide synthesis protocols (Amylin lots #CS171297 and #P180597, respectively). Amino acid compositions and purity were confirmed by amino acid analyses (average error in residue count $<6.1\pm5.9\%>$ for Glx, Asx and all residues other than Trp, $<1.7\%>$ for Asx/Glx/Pro/Gly/Met/Leu/Lys/His) and HPLC ($>98\%$ on Vydac C18). The average molecular weights observed by MS were within 0.6 amu of the expectation based on the sequence. NMR analyses[25] have confirmed the sequence and purity of the peptides. The results of one NMR experiment, an attempt to examine exendin-4 in D_2O/TFE medium after complete exchange of backbone NH signals, is pertinent to the present study. A sample of exendin-4 was dissolved in 10:1 phosphate buffered D_2O/TFE (peptide concentration 700 μM, 15 mM phosphate) with pH* adjusted to 5.35. Repeated lyophilizations (with addition of 99.9 + % D_2O buffer each time) over ca. 3 days were performed prior to preparation of the NMR sample (3:7 d_3-TFE/D_2O-buffer, pD 5.9).

CD samples were prepared by dissolving weighed amounts (0.5–2 mg) of freshly vacuum-dried peptides directly in 15 mM aqueous phosphate (pH 3.5 or 5.9) or acetate (pH 4.5) to produce stock solutions with nominal concentrations of ca. 600 μM. The concentrations of the stock solutions were determined by UV using the Trp absorbance ($\varepsilon_{278\,nm} = 5580\,cm^2/mmol$) and correcting for a non-zero baseline. For the preparation of samples in DPC micelle solutions, concentrated peptide stock solutions were prepared in 30 vol% TFE. The dilution factor into the aqueous micelle mixtures (40 mM DPC) was large, producing final TFE concentrations <2 vol%. CD spectra were recorded using a JASCO model J720 spectropolarimeter with a nitrogen flow rate of 5 L/min. The wavelength and degree ellipticity scales were calibrated using a reference d–10-camphorsulfonic acid (CSA) sample assuming that the CSA minimum corresponds to $[\theta]_{192.5} = -15{,}600$.[26] Typical spectral accumulation parameters were a time constant of 0.25 s and a scan rate of 100 nm/min with a 0.2 nm step resolution over the range 185–270 nm with 16 scans averaged for each spectrum. The accumulated average spectra were trimmed at a dynode voltage of 650 prior to baseline subtraction and smoothing using the reverse Fourier transform procedure in the JASCO software. CD spectral values for peptides are expressed in units of residue molar ellipticity (deg.cm^2/residue-dmol). Final peptide concentrations of 2-315μM in the CD cells (typically of 5 to 0.1mm path length) were obtained by quantitative serial dilution of the freshly prepared stock solutions to the required levels of fluoroalcohol and aqueous buffer (10–20 mM phosphate).

Acknowledgements

Studies at the University of Washington were supported by a grant from Amylin Pharmaceuticals, Inc. We wish to thank Ved P. Srivastava (Amylin Pharmaceuticals) and R. Matthew Fesinmeyer (University of Washington) for revision suggestions following critical readings of drafts of this manuscript.

References and Notes

1. Abbreviations used: the standard one and three letter symbols for amino acid residues are employed; $[\theta]_{221}$, the residue molar ellipticity at 221 nm (a measure of helicity); χ_{helix}, the helix mole fraction averaged over the residue span that displays some helicity based on NMR parameters or helix/coil transition simulations; pH*, pH meter reading for D_2O-containing solutions when H_2O reference buffers are employed for calibration; CD, circular dichroism; CSA, d-10-camphorsulfonic acid; DPC, dodecylphosphocholine; GLP-1, glucagon-like-peptide-1 (7- 36)-amide; HFIP, hexafluoroisopropanol; TFE, trifluoroethanol; SDS, sodium dodecylsulfate.
2. Fehmann, H. C.; Haebener, J. F. *Trends Endocrinol. Metab.* **1992**, *3*, 158.
3. Thorens, B. *Proc. Natl. Acad. Sci. U.S.A.* **1992**, *89*, 8641.
4. (a) Wettergren, A.; Schjoldager, B.; Mortensen, P. E.; Myhre, J.; Christiansen, J.; Holst, J. J. *Dig. Dis. Sci.* **1993**, *38*, 665. (b) Dupre, J.; Behme, M. T.; Hramiak, I. M.; McFarlane, P.; Williamson, M. P.; Zabel, P.; McDonald, T. J. *Diabetes* **1995**, *44*, 626.
5. Turton, M. D.; O'Shea, D.; Gunn, I.; Beak, S. A.; Edwards, C. M.; Meeran, K.; Choi, S. J.; Taylor, G. M.;

Heath, M. M.; Lambert, P. D.; Wilding, J. P.; Smith, D. M.; Ghatei, M. A.; Herbert, J.; Bloom, S. R. *Nature* **1996**, *379*, 69.
6. Bray, G. A.; Tartaglia, L. A. *Nature* **2000**, *404*, 672.
7. Eng, J.; Kleinman, W. A.; Singh, L.; Singh, G.; Raufman, J. P. *J. Biol. Chem.* **1992**, *267*, 7402.
8. Göke, R.; Fehmann, H. C.; Linn, T.; Schmidt, H.; Krause, M.; Eng, J.; Göke, B. *J. Biol. Chem.* **1993**, *268*, 19650.
9. Young, A. A.; Gedulin, B. R.; Bhavsar, S.; Bodkin, N.; Jodka, C.; Hansen, B.; Denaro, M. *Diabetes* **1999**, *48*, 1026.
10. Sasaki, K.; Dockerill, S.; Adamiak, D. A.; Tickle, I. J.; Blundell, T. *Nature* **1975**, *257*, 751.
11. Braun, W.; Wider, G.; Lee, K. H.; Wüthrich, K. *J. Mol. Bio.* **1983**, *169*, 921.
12. Epand, R. M.; Jones, A. J.; Sayer, B. *Biochemistry* **1977**, *16*, 4360.
13. Thornton, K.; Gorenstein, D. G. *Biochemistry* **1994**, *33*, 3532.
14. Parker, J. C.; Andrews, K. M.; Rescek, D. M.; Massefski, W., Jr.; Andrews, G. C.; Contillo, L. G.; Stevenson, R. W.; Singleton, D. H.; Suleske, R. T. *J. Pept. Res.* **1998**, *52*, 398.
15. (a) Muñoz, V.; Serrano, L. *Nat. Struct. Bio.* **1994**, *1*, 399. (a) Doig, A. J.; Baldwin, R. L. *Prot. Sci.* **1995**, *4*, 1325.
16. Andersen, N. H.; Tong, H. *Prot. Sci.* **1997**, *6*, 1920.
17. (a) Bruch, M. D.; Dhingra, M. M.; Gierasch, L. M. *Proteins* **1991**, *10*, 130. (b) Muñoz, V.; Serrano, L.; Jiménez, M. A.; Rico, M. *J. Mol. Bio.* **1995**, *247*, 648.
18. Luo, P.; Baldwin, R. L. *Biochemistry* **1997**, *36*, 8413.
19. Shalongo, W.; Dugad, L.; Stellwagen, E. *J. Am. Chem. Soc.* **1994**, *116*, 2500.
20. Muñoz, V.; Serrano, L. *Biopolymers* **1997**, *41*, 495 Available at http://www.embl-heidelberg.de/Services/serrano/agadir/agadir-start.html
21. Available at http://faculty.washington.edu/nielshan/
22. Adelhorst, K.; Hedegaard, B. B.; Knudsen, L. B.; Kirk, O. *J. Biol. Chem.* **1994**, *269*, 6275.
23. (a) Andersen, N. H.; Cort, J. R.; Liu, Z.; Sjoberg, S. J.; Tong, H. *J. Am. Chem. Soc.* **1996**, *118*, 10309. (b) Andersen, N. H.; Dyer, R. B.; Fesinmeyer, R. M.; Gai, F.; Liu, Z. H.; Neidigh, J. W.; Tong, H. *J. Am. Chem. Soc.* **1999**, *121*, 9879.
24. Gallwitz, B.; Witt, M.; Paetzold, G.; Morys-Wortmann, C.; Zimmermann, B.; Eckart, K.; Folsch, U. R.; Schmidt, W. E. *Eur. J. Biochem.* **1994**, *225*, 1151.
25. Neidigh, J. W. Ph.D. in Chemistry; University of Washington: Seattle, WA, 1999, pp 226.
26. Yang, J. T.; Wu, C. S.; Martinez, H. M. *Methods Enzymol.* **1986**, *130*, 208.